Acoustical Physics, Vol. 51, No. 5, 2005, pp. 543–553. Translated from Akusticheskiĭ Zhurnal, Vol. 51, No. 5, 2005, pp. 633–644.

Experimental Study of Nonlinear Acoustic Effects in a Granular Medium

V. Tournat, V. Yu. Zaĭtsev*, V. E. Nazarov*, V. É. Gusev**, and B. Castagnéde****

** Institute of Applied Physics, Russian Academy of Sciences, ul. Ul'yanova 46, Nizhni Novgorod, 603950 Russia*

e-mail: vyuzai@hydro.appl.sci-nnov.ru

*** Université du Maine, Av. O. Messiaen, 72 085, Le Mans, France*

Received August 16, 2004

Abstract—Results of a series of experimental studies of nonlinear acoustic effects in a granular medium are presented. Different effects observed in the experiments simultaneously testify that the nonlinearity of granular media is governed by the weakest intergrain contacts. The behavior of the observed dependences suggests that the distribution function of contact forces strongly increases in the range of forces much smaller than the mean force value, which is inaccessible for conventional experimental measuring techniques. For shear waves in a granular medium, the effects of demodulation and second harmonic generation with conversion to longitudinal waves are studied. These effects are caused by the nonlinear dilatancy of the medium, i.e., by the nonlinear law of its volume variation in the shear stress field. With the use of shear waves of different polarizations, the anisotropy of the nonlinearity of the medium is demonstrated. The observation of the cross-modulation effect shows that the nonlinearity-induced modulation components of the probe wave are much more sensitive to weak nonstationary perturbations of the medium, as compared to the linearly propagating fundamental harmonic. The nonlinear effects under study offer promise for diagnostic applications in laboratory measurements and in seismic monitoring systems. © *2005 Pleiades Publishing, Inc.*

1. INTRODUCTION

The development of seismoacoustic diagnostic techniques and methods of monitoring geophysical media requires knowledge of the elastic and inelastic, as well as linear and nonlinear, properties of these media and understanding of the relation between these properties and the structure of the medium; i.e., physical models of such media and the corresponding equations of state are necessary. As a rule, the chemical compositions and the physical structures of different kinds of rock are complex and diversified, which determines the wide range of acoustic properties of rocks and, hence, a rich "spectrum" of nonlinear wave processes in them. On the other hand, the variety of rocks can be separated into several classes according to their structural similarity, which determines the similarity of their acoustic properties (even for different chemical compositions). One such important class of geophysical media includes granular materials. Their specificity is primarily determined by the nonlinearity of the contacts between the grains forming a granular medium. This structural feature of granular media makes their acoustic nonlinearity qualitatively different from that of homogeneous (continuous) amorphous and crystalline solids, which makes studying the nonlinear propagation and interaction of elastic waves in granular systems particularly interesting [1]. To describe and predict the macroscopic behavior of a granular medium (with one or another packing) in the field of elastic waves, it is necessary to know the distribution of the forces f acting on the intergrain contacts. The results of both theoretical and experimental studies point to the fact that the distribution function of the contact forces, $P = P(f)$, rapidly decreases when f exceeds a certain characteristic force f_0 related to the strain of the medium [1–7]. On the other hand, there still are no commonly accepted models of the distribution $P = P(f)$ for $f < f_0$. In the literature, one can find arguments in favor of both a decrease [4] and an increase [5–7] in $P(f)$ for $f < f_0$. The existing experimental techniques [1–4] are insufficiently sensitive to allow choosing between the theories describing the distribution of weak forces ($f \ll f_0$). These techniques are based on the study of the prints of grains on a carbon paper, the use of a microbalance for measuring the normal forces acting on individual grains at the boundary of the medium, and the visualization of the deformation of grains with the help of optoelastic effects. All of these methods deal with effects that become stronger as the force f increases, so that the contribution of the most-loaded contacts to the result of measurements is predominant. Hence, it is especially important to study the aforementioned manifestations of granular media by experimental methods in which the response of weak contacts is greater than that of strong contacts. Such methods can be developed on the basis of nonlinear acoustic effects, which are sensitive to the weakest mechanical contacts and defects in the structure of the medium [8–11]. In contrast to the

1063-7710/05/5105-0543$26.00 © 2005 Pleiades Publishing, Inc.

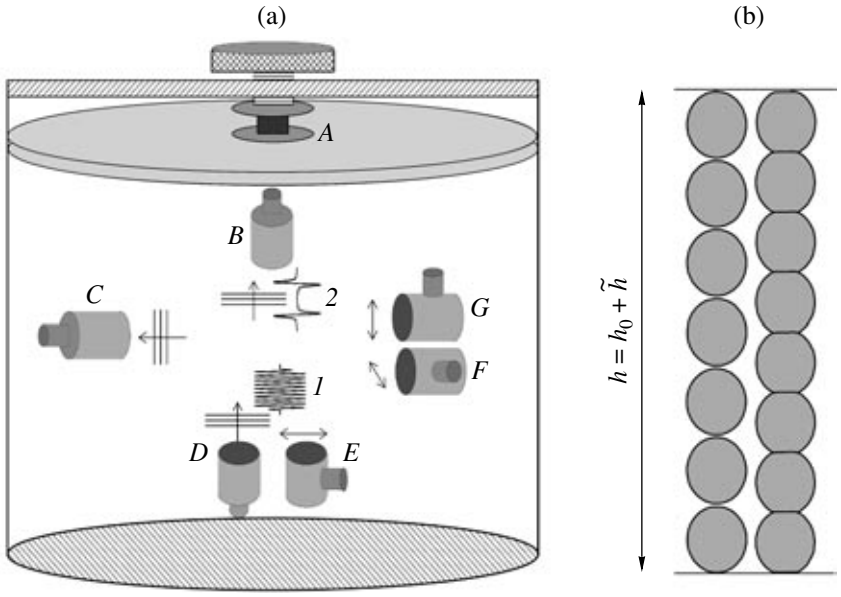

Fig. 1. (a) Experimental setup and (b) a schematic representation of two grain chains of a granular medium with different static compressions: (*A*) control dynamometer, (*B*, *C*) receiving transducers, (*D*) longitudinal wave radiator, and (*E*–*G*) transverse wave radiators with different wave polarizations.

known approaches [1–4], nonlinear acoustic methods, in principle, allow one to obtain information on the distribution function $P = P(f)$ in the bulk of the medium (rather than at its boundary) for the range of forces $f < 5 \times 10^{-2} f_0$.

In this paper, we combine and discuss from a single point of view the results of a series of experimental studies of the effects associated with the nonlinear propagation and interaction of longitudinal (L) and shear (S) elastic waves in granular media. The intensity of these effects mainly depends on the nonlinearity of weak intergrain contacts, which determine the acoustic nonlinearity of the medium as a whole. We consider demodulation effects, second harmonic generation for high-frequency (HF) pulses, and cross-modulation of a weak (probing) harmonic wave under the effect of an intense amplitude-modulated pump wave.

2. ELASTIC NONLINEARITY OF A GRANULAR MEDIUM

Let us discuss the origin of the high sensitivity of nonlinear acoustic effects in a granular medium to the presence of weak intergrain contacts. As is known, the origin of the strong elastic nonlinearity of a granular medium is the Hertzian nonlinearity of contacts between the grains [12]. For a medium with uniformly loaded contacts, this nonlinearity leads to the following equation of state, i.e., to the dependence $\sigma = \sigma(\varepsilon)$:

$$\sigma(\varepsilon) = bn\varepsilon^{3/2}H(\varepsilon), \tag{1}$$

where σ and ε are the stress and strain, the factor b depends on the elastic moduli of the grain material, n is the average number of contacts per grain, and $H(\varepsilon)$ is the Heaviside function showing that stress occurs in the medium only when the contacts are under compression ($\sigma, \varepsilon > 0$). An actual granular medium contains contacts with different loads [1–8], which requires a modification of Eq. (1). To reveal the role of different contacts in acoustic manifestations, we assume that a granular medium contains only two fractions of contacts with different static strains. Separating the static (σ_0, ε_0) and dynamic ($\tilde{\sigma}$, $\tilde{\varepsilon}$) components of stress and strain for both fractions, we obtain the following equation from Eq. (1):

$$\begin{aligned}\sigma_0 + \tilde{\sigma} &= bn_1(\varepsilon_0 + \tilde{\varepsilon})^{3/2}H(\varepsilon_0 + \tilde{\varepsilon}) \\ &+ bn_2(\mu\varepsilon_0 + \tilde{\varepsilon})^{3/2}H(\mu\varepsilon_0 + \tilde{\varepsilon}),\end{aligned} \tag{2}$$

where n_1 and n_2 are the average numbers of contacts per grain for the two fractions and μ is the dimensionless parameter characterizing the weak ($\mu \ll 1$) static strain of grains of the second fraction compared to that of the first fraction. Note that the dynamic strain $\tilde{\varepsilon}$ is the same for both fractions. This can be explained by considering the deformation of loaded grain chains shown in Fig. 1. Assume that, under the effect of dynamic stress, the chain length h oscillates around its mean value h_0 ($h = h_0 + \tilde{h}$, $|\tilde{h}| \ll h_0$). Then, the strain of the chain consisting of N grains with a diameter d will be equal to $\varepsilon = (Nd - h_0 - \tilde{h})/Nd$. Consider a chain that has a zero strain in the absence of acoustic load and assume that this chain has a number of grains equal to $N_0 = h_0/d \gg 1$. Taking the number of grains in the ith chain to be $N_i =$

$N_0 + \Delta N_i$, where $\Delta N_i \ll N_0$, we find that the strain ε_i determined as the sum of the static and dynamic components is approximately $\varepsilon_i \cong \Delta N_i/N_0 + \tilde{h}/h_0$. Correspondingly, the dynamic strain component $\tilde{\varepsilon} = \tilde{h}/h_0$ will be the same for all of the grains belonging to different chains. By contrast, the static strains $\varepsilon_0^{(i)} = \Delta N_i/N_0$ ($i = 1, 2$) are different for different chains, because $\Delta N_1 \neq \Delta N_2$. Note that the difference in the static strains $\varepsilon_0^{(i)}$ for these chains can be relatively large even for $\Delta N_i/N_0 \ll 1$. Evidently, the model of the medium presented above is quasi-one-dimensional, and it assumes that the more neavily loaded grain chains relieve other grains from the load. In actual three-dimensional packings, it is possible to single out similar, predominantly loaded, quasi-one-dimensional grain chains, so that, in an actual medium, the dynamic strain can be considered as identical for all contacts to a first approximation. Then, at $n_1 \sim n_2$, we obtain that the first (more strained) fraction in Eq. (1) carries the major part of the static load applied to the medium. For this fraction, the strain $\varepsilon_0^{(1)} = \Delta N_1/N_0$ approximately corresponds to the strain of the medium ε_0. Thus, in terms of the static strains of different contact fractions, the compliance parameter of the ith fraction is determined by the ratio: $\mu^{(i)} = \varepsilon_0^{(i)}/\varepsilon_0$.

For preliminarily compressed contacts and moderate dynamic strains $|\tilde{\varepsilon}| \ll \mu\varepsilon_0$, Eq. (2) can be expanded into a Taylor series with coefficients $d^m\tilde{\sigma}(\varepsilon_0)/d\tilde{\varepsilon}^m$. These coefficients characterize the linear ($m = 1$) and nonlinear ($m = 2, 3, \ldots$) elastic moduli M_m of the medium, which determine the velocity of acoustic wave propagation, the nonlinear correction to it, and the intensity of nonlinear effects of the mth order:

$$M_m \sim \frac{d^m\tilde{\sigma}(\varepsilon_0)}{d\tilde{\varepsilon}^m} \sim bn_1\left(1 + \frac{n_2}{n_1}\mu^{(3/2)-m}\right)\varepsilon_0^{(3/2)-m}. \quad (3)$$

Expression (3) shows that the contribution made by the weak contacts to the linear modulus M_1 is proportional to $\mu^{1/2} \ll 1$ and is negligibly small at $n_1 \sim n_2$. By contrast, the contribution of the weak fraction to the nonlinear moduli M_m ($m = 2, 3, \ldots$) is proportional to $\mu^{(3/2)-m} \gg 1$ and, hence, predominates in the presence of sufficiently small static strains $\mu \leq 10^{-1}$–10^{-2}. Such strains correspond to still smaller forces $f/f_0 \leq 3 \times 10^{-2}$–$10^{-3} \ll \mu$, which fall beyond the sensitivity range of the known experimental techniques [1–4].

From Eq. (3), it follows that, in the case of the demodulation of weak HF acoustic pulses with an amplitude $\varepsilon_p < \mu\varepsilon_0$, when the power series expansion of Eq. (2) is valid, the amplitude $\in_{\text{det}}$ should be quadratic in ε_p: $\in_{\text{det}} \sim M_2\varepsilon_p^2$. For higher amplitudes ($\varepsilon_p > \mu\varepsilon_0$), with allowance for the fact that the nonlinearity in Eq. (2) is governed by the second term, the amplitude $\in_{\text{det}}$ is determined by the expression: $\in_{\text{det}} \sim \langle\tilde{\varepsilon}^{3/2} H(\tilde{\varepsilon})\rangle \sim \varepsilon_p^{3/2}$. This means that the dependence of $\in_{\text{det}}$ on ε_p should exhibit a transition from the square law to the 3/2-power law. Such a transition testifies that weak contacts with $\mu \sim \varepsilon_p/\varepsilon_0 \ll 1$ are present in the medium. Similar speculations are valid for the amplitude dependence of the nonlinear sources producing the second-harmonic wave in the medium.

3. EXPERIMENTAL SETUP

The experimental setup for studying the nonlinear acoustic effects in a granular medium is shown in Fig. 1. The granular medium was composed of glass beads 2 mm in diameter, which filled a cylindrical container with a diameter of 40 cm and a height of 50 cm. The vertical static load was produced by a rigid piston and controlled by an electronic dynamometer. The static stresses and strains could be varied within 10–50 kPa and $(1–5) \times 10^{-4}$, respectively. Piezoelectric transducers were used to excite intense longitudinal and shear waves in the pulsed or continuous modes (the diameter of the transducers was about 4 cm). The receivers of acoustic (strain) waves transmitted through the medium were piezoelectric transducers with a longitudinal polarization (of the same type as those used for the emission of longitudinal waves). The positions and polarization of acoustic radiators and receivers in the container are shown in Fig. 1.

4. DEMODULATION OF A HIGH-FREQUENCY S WAVE WITH A CONVERSION INTO A LOW-FREQUENCY L WAVE

In the first experiment [13], primary HF pulses (with a carrier frequency of 30–80 kHz) with longitudinal and transverse polarizations were excited in the medium. Because of the strong absorption in the granular medium, these pulses rapidly decayed (within a distance of 5 cm). As a result of the demodulation (rectification) of these pulses in the medium because of the Hertzian nonlinearity of the contacts, secondary low-frequency (LF) longitudinal pulses (with a characteristic frequency of 4–6 kHz determined by the steepness of the leading edges of the primary HF pulses) were generated in the medium and propagated through it. In hydroacoustics, devices whose operation is based on this principle are called parametric radiators [14]; in this case, both primary and secondary waves are assumed to be longitudinal. The operation of parametric radiators with a shear pump wave is possible in a granular medium because of its dilatancy [15, 16], i.e., the ability of the granular medium to expand under shear stresses. This leads to a nonlinear transformation of the signal frequency with a simultaneous change of the wave polarization (i.e., an amplitude-modulated HF S pump wave is transformed into a demodulated LF L

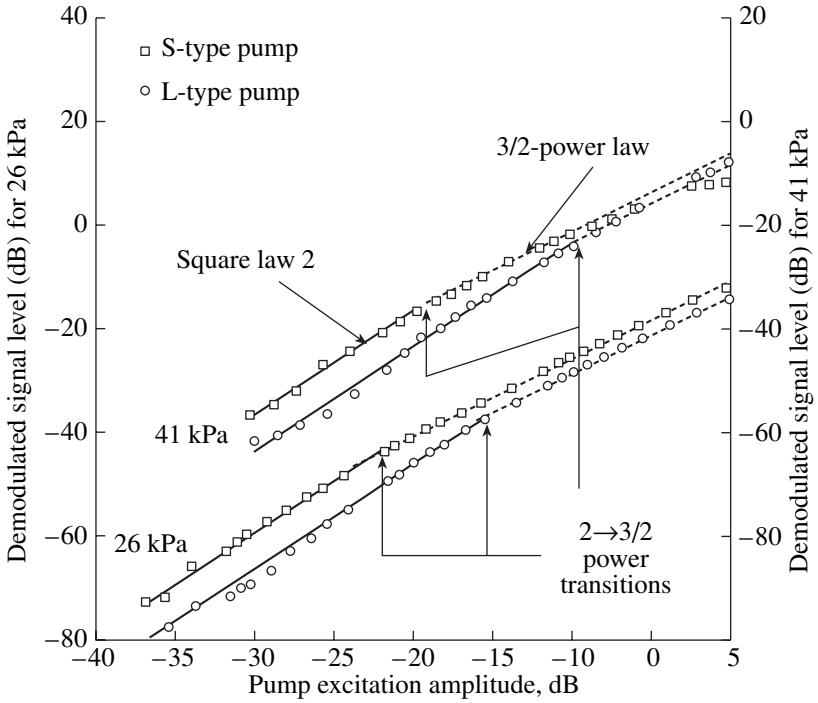

Fig. 2. Demodulated signal amplitude as a function of the excitation amplitude of vertically propagating S and L pump waves for two static pressures.

wave). Generally speaking, the effect of demodulation of HF acoustic pulses with a conversion from S to L waves is also possible in a homogeneous medium with a quadratic elastic nonlinearity [17]. However, because of the noticeable difference in the propagation velocities of the primary S wave and the secondary L wave (when the dissipation in the medium is relatively weak), their interaction will be asynchronous and the amplitude of the demodulated signal will experience spatial beatings.

In the given experiment, relatively long HF pulses with a rectangular envelope were emitted, so that the demodulated LF pulses from the leading and trailing edges of the primary HF pulses did not overlap and could be observed separately. With the chosen parameters of HF pulses and pump transducer dimensions, the demodulation of the signal occurred for a highly directional primary wave [14]. In this case, the shape of the demodulated strain pulses corresponded to the second derivative of the HF pulse envelope with respect to time. Figure 2 shows examples of the dependences of the amplitude $\in_{\text{dem}}$ of the demodulated pulses on the amplitude ε_p of the primary L and S pulses (for different values of static pressure). The strain level in the pump wave (in its whole range) remained below the initial static strain of the medium.

From the amplitude dependences obtained for the demodulated pulses (Fig. 2), one can see that their main feature (for both L and S pump pulses) is as follows: for small amplitudes ε_p of the primary pulse, a quadratic dependence of the amplitude $\in_{\text{dem}}$ on ε_p is observed, and for large primary pulse amplitudes, this dependence exhibits a transition to a 3/2-power law, which corresponds to the Hertzian nonlinearity. It should be stressed that this transition occurs when the strain amplitude ε_p is 15–20 dB lower than the static strain ε_0. As it was noted above, the 3/2-power-law amplitude dependence is typical of weak "clapping" contacts, and the predominance of this dependence for $\varepsilon_p \ll \varepsilon_0$ testifies to a considerable growth of the distribution function $P = P(f)$ in the range of small contact forces (below several percent of their mean value f_0). Here, it should be taken into account that, in terms of the introduced notations, the following relation is valid for Hertzian contacts: $f/f_0 \sim \mu^{3/2} \ll 1$. This allows one to relate the distribution function $P = P(f)$ to the contact strain distribution $n = n(\mu)$ or vice versa, by taking into account the relation $P(f)df = n(\mu)d\mu$, so that, if, e.g., $n(\mu) = \text{const}$, one obtains $P(f) \sim f^{-1/3}$. Concerning the behavior of the function $P = P(f)$, many publications argue that the distribution of contact forces for $f < f_0$ has a fairly flat plateau $P(f) \approx \text{const}$ [2, 3, 5, 6]. However, it can be easily shown that such an assumption is inconsistent with the observed dependence of $\in_{\text{det}}$ on ε_p. Moreover, even assuming that $P(f) \sim f^{-1/3}$, which corresponds to $n(\mu) = \text{const}$ in Eq. (2), one can see that the power law $P(f) \sim f^{-1/3}$ (for small f) is insufficient to obtain the transition from power 2 to power 3/2 observed in the dependence of $\in_{\text{dem}}$ on ε_p. A calculation showed (see Fig. 3a) that, in the case of a uniform dis-

tribution of contacts in the initial strain $n(\mu) = \text{const}$ (i.e., for the distribution of the form $P(f) \sim f^{-1/3}$ in terms of contact forces), despite the discontinuities (clapping) of the weak contacts, the amplitude $\in_{\text{dem}}$ almost quadratically depends on ε_p in the whole range of the pump amplitude up to its value equal to the mean static strain of the material, $\varepsilon_p \sim \varepsilon_0$. Indeed, in the case of the distribution $n(\mu) \approx \text{const}$, the number of clapping contacts increases with increasing ε_p. As a result, the amplitude of the demodulated pulse grows faster than $\varepsilon_p^{3/2}$ and the amplitude dependence of this pulse remains close to quadratic one as long as $\varepsilon_p/\varepsilon_0 \le 1$. It is only when $\varepsilon_p/\varepsilon_0 > 1$ that almost all contacts begin clapping and the quadratic dependence passes into $\in_{\text{dem}} \sim \varepsilon_p^{3/2}$. Thus, the transition from the 2-power law to the 3/2-power law in the amplitude dependence of the demodulated signal observed in the experiment for $\varepsilon_p/\varepsilon_0 \ll 1$ testifies to the presence of a considerable fraction of weak contacts (with $\mu \sim 10^{-1}$ or less). We stress that, for the realization of the $2 \longrightarrow 3/2$ transition in the power law characterizing the amplitude dependence of the demodulated signal, it is necessary to have a sufficiently large total number of clapping contacts with $\mu \ll \varepsilon_p/\varepsilon_0$. Hence, to model the effect of this group of contacts, it is sufficient to complement the smooth function $n(\mu) = \text{const}$ with a fraction of weak contacts concentrated in the region $0 \le \mu \le \mu_0 \ll 1$ (see the example in Fig. 3b, where we chose $\mu_0 = 10^{-1}$, while the total number of contacts remained the same as in Fig. 3a). In this case, the change in the power law is evident as early as at $\varepsilon_p/\varepsilon_0 \ll 1$. A similar pronounced $2 \longrightarrow 3/2$ transition in the power law of the amplitude dependence (Fig. 3b) can also be obtained when the function $n = n(\mu)$ increases smoothly but fairly rapidly, for example, when $n(\mu) \sim \mu^{1/2}$ for $0 < \mu < 1$. A more detailed reconstruction of the function $n = n(\mu)$ for $\mu \ll 1$ is difficult because of the integral character of its manifestation, but the pronounced $2 \longrightarrow 3/2$ power-law transition observed at $\varepsilon_p \sim 10^{-1}\varepsilon_0$ testifies that the growth of the contact force distribution function in the region of $f/f_0 \ll 1$ is substantial and allows one to estimate the fraction of the weak contacts belonging to this region. Note that, for the predicted $2 \longrightarrow 3/2$ transition to agree with experimental results, the characteristic value μ_0 (below which a considerable part of weak contacts is concentrated and the distribution function exhibits a sharp growth) should be not too small. Otherwise, for example, at $\mu_0 = 10^{-2}$, the $2 \longrightarrow 3/2$ transition would be observed at a much smaller value of ε_p than that obtained from the experiment.

Studying the polarization of the demodulated LF pulses, we found that it was longitudinal for both longitudinal and transverse polarizations of the HF pump wave. In addition, the propagation velocity of these pulses, which was determined from the arrival time,

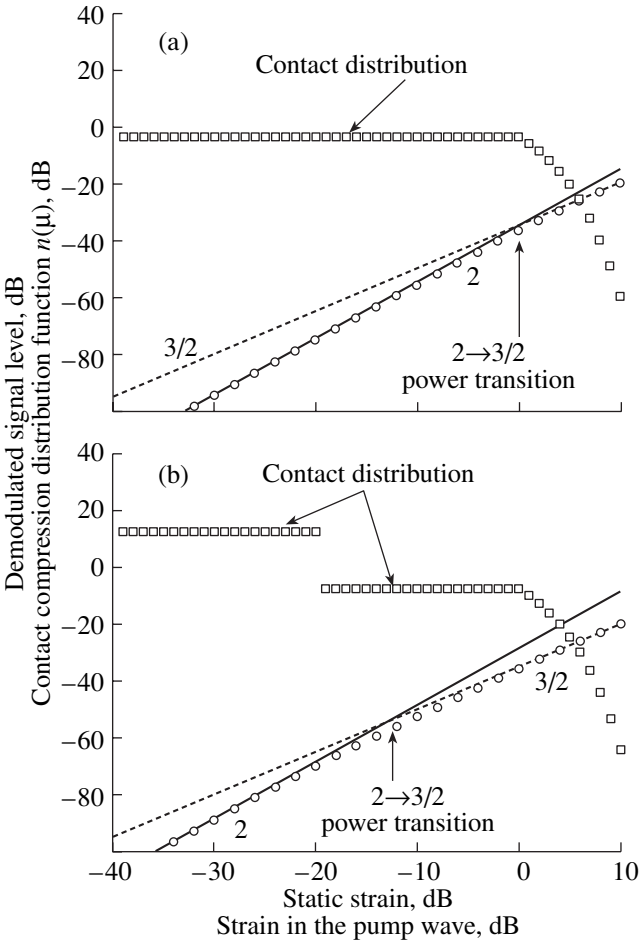

Fig. 3. Demodulated signal level $\in_{\text{dem}}$ (circles) modeled as a function of pump amplitude ε_p for different contact compression distribution functions $n(\mu)$ (squares): (a) $n(\mu)$ in the form of a flat plateau, $n(\mu) = \text{const}$, for $0 \le \mu \le 1$; (b) $n(\mu)$ in the form of a plateau with an additional weak contact fraction containing about 50% of the total contact number in the region $0 \le \mu \le \mu_0 = 10^{-1}$. The value of 0 dB on the abscissa axis corresponds to the static strain of contacts with $\mu = 1$, i.e., to the initial static strain of the medium.

was also close to the propagation velocity of the L wave. Figure 4 shows the shapes of the LF pulses for two different frequencies of the S pump wave. When the frequency of the S pump wave was reduced, the decrease in its attenuation caused an increase in the length of the nonlinear interaction region, where the nonlinear source propagated with the velocity of the S wave. This caused a noticeable additional delay of the demodulated pulses and an increase in their duration, which was not observed in the case of L pump pulses.

As noted above, the conversion of a shear wave into a demodulated longitudinal wave occurs owing to the dilatancy phenomenon (an increase in the volume of the medium under the effect of a shear). Therefore, the dependence of the demodulated pulse amplitude $\in_{\text{dem}}$ on the shear pump amplitude ε_p provides the information on the character of the dynamic (i.e., caused by the

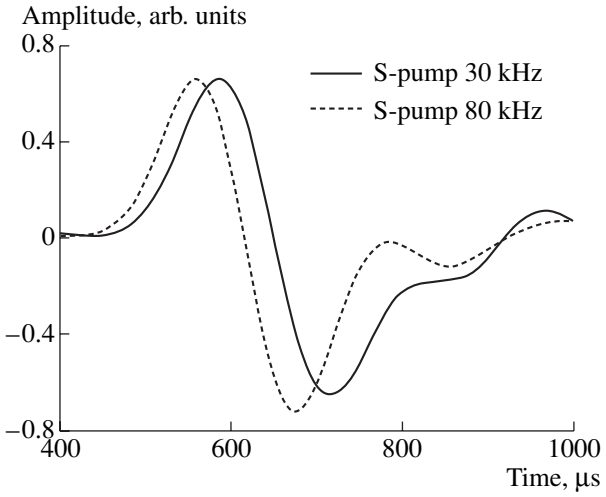

Fig. 4. Examples of the shapes of the received demodulated pulses for the longitudinal mode and two frequencies of the shear pump wave. For a pump frequency of 30 kHz, the additional delay in the first maxima is 26 ± 1 μs and the pulse broadening (between the extrema) is 14 ± 1 μs, as compared to the case of a pump frequency of 80 kHz.

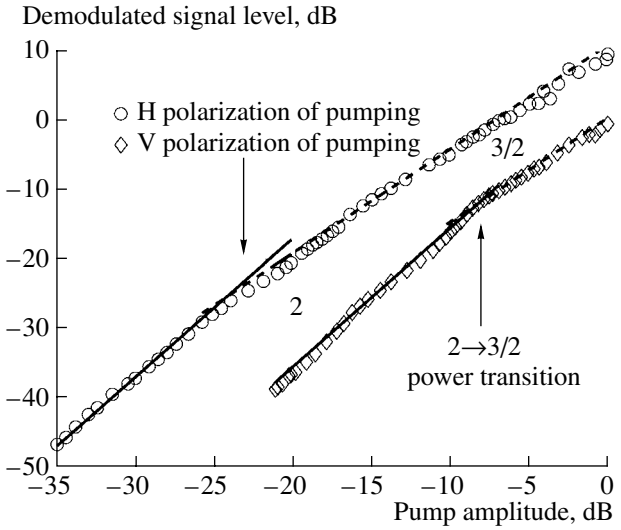

Fig. 5. Demodulated signal amplitude as a function of the amplitude of the S pump wave for the case of its horizontal propagation with (V) vertical and (H) horizontal polarizations (the pressure on the medium is 64 kPa). The characteristic amplitudes corresponding to the 2 ⟶ 3/2 power transition are indicated by arrows.

shear acoustic wave) dilatancy of the medium. The classical dilatancy of a granular medium (according to Reynolds) can be qualitatively understood from kinematic considerations [15] as the combination of slip and rotation of the initially closely-packed grains with respect to each other, which leads to an increase in the volume of the medium. Both the kinematics of incompressible grains [15, 16] and the linearized hyperplasticity equations [18] predict a volume expansion of a granular medium in direct proportion to the shear stress amplitude. Such a dilatancy law leads to a linear dependence of $\in_{\text{dem}}$ on ε_p (note that the stress and strain in an acoustic wave are proportional to each other in the first approximation). However, at small amplitudes, the experimental dependence of $\in_{\text{dem}}$ on ε_p is quadratic and, as the pump amplitude increased (up to $\varepsilon_p \sim \varepsilon_0 \sim (1\text{–}5) \times 10^{-4}$), passed to the 3/2-power law, which corresponds to the nonlinearity of clapping Hertzian contacts. Thus, in the presence of small (acoustic) strains, the dilatancy of a granular medium noticeably manifests itself and is primarily related to the compressibility of the intergrain contacts rather than to the kinematic effects of a repacking of grains.

The effect of demodulation of shear waves with different polarizations can also be used for determining the anisotropy of the contact nonlinearity of the granular medium and for revealing the force chains preliminarily oriented along the static stress in the medium. Indeed, since the contact nonlinearity is inversely proportional to the static strain (Eq. (3)), a medium with an anisotropy of contact loads should have different nonlinearities for shear waves of different polarizations. Figure 5 shows examples of the amplitude dependences of demodulated pulses originating from identical horizontally directed S pump radiators with vertical (V) and horizontal (H) polarizations. From these dependences, one can see that, first, in the case of an H-polarized pumping, the demodulated pulse amplitude is approximately 10 dB higher than that in the case of the V-polarized pumping; second, the transition to clapping contacts (2 ⟶ 3/2) for H-polarized pumping is observed at amplitudes 7–12 dB lower than that for V-polarized pumping. These facts testify that the nonlinear elastic parameters of a granular medium are different for the H- and V-polarized shear pump waves; i.e., an anisotropy of nonlinearity occurs in the medium, because the horizontal contacts are loaded less than the vertical ones. In connection with this, we note that the propagation of an HF harmonic S pump wave with a circular polarization of frequency Ω in such a medium may be accompanied by the effect of generation of LF L waves with frequencies $2k\Omega$, where $k = 1, 2, \ldots$. The amplitude dependences and the amplitude ratios of these waves characterize the dynamic dilatancy law and the anisotropy of the acoustic nonlinearity of a granular medium.

5. SECOND HARMONIC GENERATION FOR AN L WAVE UNDER AN S PUMP WAVE

The second harmonic generation is a classical nonlinear effect that is widely used, for example, in optics for the radiation frequency conversion and in nonlinear acoustics for nondestructive testing of materials. The efficiency of the conversion of the fundamental harmonic to the second one depends on the nonlinear

parameters and dispersion of the medium. The latter determines the possibilities for a synchronous accumulation of the nonlinear effect. In dispersive media, the phase velocities of waves with frequencies ω and 2ω differ from each other, and the dependence of the second harmonic amplitude on distance exhibits oscillations (beatings). For acoustic waves, the dispersion is usually weak and only manifests itself in certain specific cases, for example, in acoustic waveguides [19]. Below, we describe the observation of such beatings for the second harmonic generation in a granular medium [20]; however, these beatings are characterized by some distinctive features. First, the lack of synchronism between the primary pump wave and the second harmonic is in this case related not to the dispersion of a single type of waves but to the velocity difference arising with the nonlinear conversion of the S wave of frequency ω into the L wave of frequency 2ω. (In homogeneous solids, such a process is virtually unobservable because of the large difference between the longitudinal and shear wave velocities and because of the small value of the nonlinear parameter.) Second, beatings of the second harmonic amplitude were observed not with an increase in distance but with an increase in the amplitude of the primary S wave, which is related to the nonlinear transformation in the wave interaction region.

In the experiment, the frequency of the horizontally propagating S pump wave was $f = 5.12$ kHz (the wavelength was $\lambda \approx 4$ cm), and its polarization could be either vertical or horizontal. The distance from the radiating transducers to the receiver was $R \approx 16$ cm. For a transducer with a radius of $a \approx 2$ cm, the diffraction length was $L_d \sim \pi a^2/\lambda \sim 3$ cm, so that the second harmonic generation mainly occurred in the region of the spherical divergence of the pump wave. Here, as in the case of demodulation, the generation of the second harmonic for the S wave is accompanied by a conversion to the L wave.

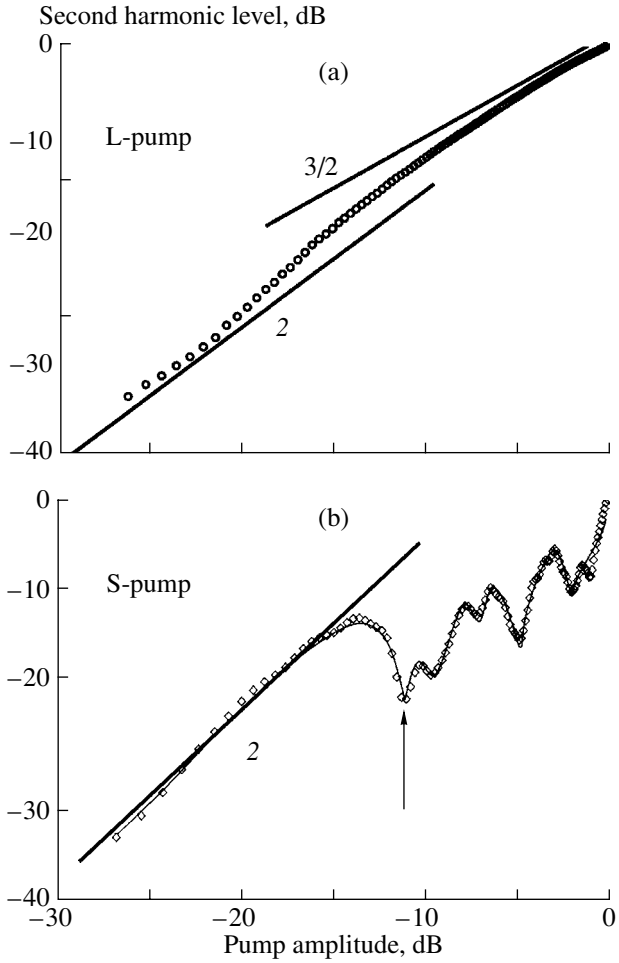

Fig. 6. Examples of the second harmonic level, measured for the longitudinal mode, as a function of the amplitude of the horizontally propagating (a) L pump wave and (b) V-polarized S pump wave. The straight lines represent the square power law and the 3/2 power law (the powers are indicated near the lines).

Figure 6 shows examples of the observed dependences of the second harmonic amplitudes received in the longitudinal mode on the amplitudes of a longitudinal pump wave and a V-polarized shear pump wave (at a static pressure of 41 kPa). From Fig. 6a, one can see that, in the amplitude dependence obtained for a longitudinal pump wave, beatings are absent and the behavior of the second harmonic amplitude is similar to the behavior of the amplitude of a demodulated pulse (see Fig. 2); i.e., a $2 \longrightarrow 3/2$ transition is observed in the power-law dependence. For the shear pumping case (Fig. 6b), the behavior of the second harmonic amplitude is qualitatively different: instead of the monotonic $2 \longrightarrow 3/2$ transition, the power law exhibits pronounced beatings. In Fig. 6, the level of 0 dB on the abscissa axis corresponds to the maximum strain amplitude of the pump wave $\varepsilon_p \approx 1.4 \times 10^{-5}$, which is more than an order of magnitude smaller than the static strain of the medium (2.4×10^{-4} at a static pressure of 41 kPa). As the static pressure increases, the position of the first minimum of the second harmonic amplitude (indicated by the arrow in Fig. 6b) is shifted toward higher pump amplitudes.

As in the demodulation experiments described above, the use of shear pump waves of different polarization made it possible to observe the effect of anisotropy of the medium by comparing the dependences of the second harmonic amplitude on the amplitudes of horizontally propagating H- and V-polarized S pump waves. The comparison of these dependences showed that, under the same static pressure, for the H- polarized wave, the second harmonic level was higher (typically, by 5–10 dB) and the beatings began at lower (also by 5–10 dB) pump amplitudes, as compared to those for the V-polarized wave. This result agrees well with analogous observations for the demodulation effect.

The beatings observed with varying amplitude of the S pump wave were related to the fact that, in the

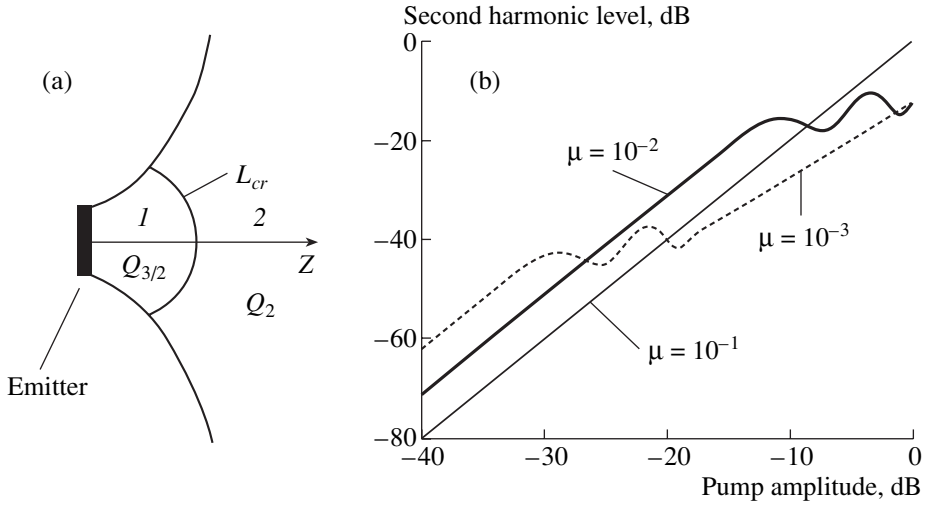

Fig. 7. (a) Schematic representation of the clapping ($Q_{3/2}$) and square-law (Q_2) modes of nonlinear sources in the second harmonic generation region and (b) dependences of the second harmonic amplitude on the pump amplitude modeled on the basis of integral (6) for different values of the compliance parameter μ of the additional weak contact fraction.

region of second harmonic generation, an increase in the pump amplitude was accompanied by a change in the conditions of wave interaction. As we have noted above, the contribution of the unloaded contact fraction to the demodulated signal is predominant, and part of the weak contacts may pass to the clapping mode and make a contribution to the second harmonic so that this contribution proves to be comparable to (or even greater than) the contribution from the contacts that remain closed during the whole period of pump oscillation.

The process of the second harmonic generation in the propagation of a longitudinal harmonic pump wave is described by the integral [14]

$$\sigma^{nl}(\mathbf{r}) = \mathrm{Re}\frac{1}{4\pi}\int Q(\mathbf{r}')\frac{\exp[i\mathbf{k}_{\mathrm{rad}}(\mathbf{r}-\mathbf{r}')]}{|\mathbf{r}-\mathbf{r}'|}d^3\mathbf{r}', \quad (4)$$

where σ^{nl} and k_{rad} are the stress and the wave vector of the secondary wave and the integration is performed over the volume occupied by the nonlinear sources $Q(\mathbf{r}') \equiv Q(x', y', z')$ produced by the primary pump wave; $\mathbf{r}$ represents the coordinates of the observation point. (For a medium with a quadratic nonlinearity, $Q(\mathbf{r}') \sim \mathrm{Re}[(\varepsilon_p/2)\exp(-i\omega t + ikr')]^2$.) A similar integral can describe the generation of an L wave of frequency 2ω in the field of an intense S wave of frequency ω in a granular medium. However, in this case, it is necessary to take into account the velocity difference between the S and L waves and the specific feature of the granular medium, namely, the $2 \longrightarrow 3/2$ transition in the power law characterizing its nonlinearity.

From the study of the demodulation effect, it was found that the nonlinearity of a granular medium is quadratic only for small amplitudes ε_p of the pump wave, as long as $\varepsilon_p/\varepsilon_0 \ll \mu$; in this case, the source Q in Eq. (4) is also quadratic: $Q = Q_2 \sim (3/16)(\mu\varepsilon_0)^{-1/2}\varepsilon_p^2$. As the pump amplitude increases up to $\varepsilon_p/\varepsilon_0 > \mu$, the Hertzian nonlinearity becomes clapping, which leads to the following expression for the source: $Q = Q_{3/2} \sim (3/4\pi)\varepsilon_p^2$. At some distance L_{cr} from the pump radiator, the amplitudes of these sources coincide at the amplitude value $\varepsilon_p^{cr} \approx 16\mu\varepsilon_0/\pi^2$, which can be considered as the characteristic pump amplitude corresponding to the $2 \longrightarrow 3/2$ transition in the power law. In this approximation, Eq. (4) falls into two integrals corresponding to the square-law and clapping (3/2-power-law) modes of the sources:

$$\varepsilon^{2\omega}(\mathbf{r}) \sim \mathrm{Re}\frac{1}{4\pi}\left\{\int\limits_{r'<L_{cr}} Q_{3/2}\frac{\exp[i\mathbf{k}_{\mathrm{rad}}(\mathbf{r}-\mathbf{r}')]}{|\mathbf{r}-\mathbf{r}'|}d^3\mathbf{r}' + \int\limits_{r'>L_{cr}} Q_2\frac{\exp[i\mathbf{k}_{\mathrm{rad}}(\mathbf{r}-\mathbf{r}')]}{|\mathbf{r}-\mathbf{r}'|}d^3\mathbf{r}'\right\}, \quad (5)$$

where $\varepsilon^{2\omega}$ is the strain in the wave of frequency 2ω. Schematically, these subregions are shown in Fig. 7a. At a small pump amplitude ε_p, the region of clapping sources can still be absent. As the pump amplitude grows, such a region appears near the transducer and then moves into the depth of the medium, so that the distance L_{cr} is determined by the condition of equal amplitudes of the sources in the closed and clapping modes: $\varepsilon_p(r = L_{cr}) = 16\mu\varepsilon_0/\pi^2$. From this equality and from the condition that the pump wave be spherically divergent (i.e., $\varepsilon_p(r) \approx \varepsilon_p(r = 0)L_d/r$) in the major part of the interaction region, we obtain $L_{cr} \approx \pi^2 L_d\varepsilon_p(0)/(16\mu\varepsilon_0)$. Performing the integration across the pumping beam

and assuming that $|r' - r| \sim r$ in the denominator of integral (5), we arrive at the expression

$$\varepsilon^{2\omega}(R) \sim \mathrm{Re}\left\{\frac{\varepsilon_p^{3/2}(0)}{\pi\sqrt{L_d}}\int_{L_d}^{L_{cr}}\frac{\exp(i\Delta kz')}{(z')^{1/2}}dz' + \frac{\varepsilon_p^2(0)}{4(\mu\varepsilon_0)^{1/2}}\int_{L_{cr}}^{R}\frac{\exp(i\Delta kz')}{z'}dz'\right\}, \quad (6)$$

where $\Delta k = k - k_{\mathrm{rad}}$.

In Fig. 7b, integral (6) is represented as a function of the pump amplitude $\tilde{\varepsilon}_a$ for several values of the parameter μ characterizing the degree of unloading of the weak contacts and for other parameters corresponding to the experimental conditions (the S and L wave velocities $c_S = 225$ m/s and $c_L = 335$ m/s, respectively; $\Delta k = 95$ m^{-1}). The amplitude $\varepsilon_p^{\max}(0)$ corresponding to the level of 0 dB was chosen to be an order of magnitude smaller than the static strain ε_0. The behavior of the second harmonic amplitude shown in Fig. 7b for the same pump amplitude range as in the experiment strongly depends on the parameter μ characterizing the reduced strain of the weak contact fraction. Specifically, the initial quadratic growth and the subsequent harmonic amplitude oscillations corresponding to $\mu \sim 10^{-2}$ in the calculated plot are close to the behavior observed in the experiment.

The difference in the effective interaction lengths L_{eff} corresponding to the adjacent extrema in the second-harmonic amplitude dependence can be estimated as $\Delta z = \pi/\Delta k \sim 3.3$ cm. As the pump amplitude grows, the boundary L_{cr} of the $2 \longrightarrow 3/2$ transition in the power law describing the amplitude dependence of the demodulated signal is gradually displaced. Hence, at an observation distance of $R \sim 16$ cm, the maximum number of possible extrema can be estimated as $R/\Delta z \sim 4$–5, which agrees well with the experiment. The following increase in the effective length of the antenna array will cause no new extrema, because, within the entire distance from the emitter to the receiver, the nonlinear sources will mainly be in the clapping mode corresponding to the harmonic amplitude dependence $\sim\varepsilon_p^{3/2}$. In Fig. 7b, such a situation is illustrated by the curve corresponding to the choice of $\mu = 10^{-3}$. On the other hand, if the parameter μ is too large ($\mu = 10^{-1}$ in Fig. 7b), in the given range of pump amplitudes, the number of clapping contacts will be small and their contribution (and, hence, the change in the effective length of the array) will be too small, so that the beatings will be absent and the harmonic amplitude dependence will be quadratic. Note that, to simplify the model calculations, we used a simple approximation of the distribution function (the same parameter μ for all unloaded contacts), which already allowed us to illustrate the role of unloaded contacts in the beating effect. Thus, the nonmonotonic behavior of the second harmonic generated by a shear pump wave proves to be a sensitive indicator of the presence of weak contacts in a granular medium.

6. CROSS-MODULATION EFFECT AND ITS SENSITIVITY TO STRUCTURAL PERTURBATIONS OF THE GRANULAR MEDIUM

In addition to the aforementioned effects related to nonlinear frequency transformations toward higher and lower frequencies, we also performed experimental observations of the nonlinear acoustic response of a granular medium to transient processes induced by short pulsed actions with the use of the less common effect of amplitude modulation transfer from an intense amplitude-modulated pump wave to a probe wave of another frequency [11]. This effect is an acoustical analog of the Luxemburg–Gorki effect [21] observed in the radio wave interaction in the ionosphere. A similar effect of amplitude modulation of a weak seismoacoustic wave under the effect of an intense amplitude-modulated wave was observed in sandy soil [22]. In the model experiments described below, the effects in a granular medium were studied using an experimental setup similar to that shown in Fig. 1. A more detailed description of the experimental technique and the experimental results can be found in [23, 24].

In addition to the results considered in [23, 24], we present another typical example illustrating the great difference between the sensitivity of the fundamental component of the probe wave to the structure of the medium and the corresponding sensitivity of the first- and second-order cross-modulation components arising in the course of its propagation. In the experiment, a monochromatic probe wave with a frequency of 10 kHz and a 100% amplitude-modulated pump wave with a carrier frequency of 7 kHz and a modulation frequency of 30–40 Hz were emitted into the medium. These waves could be either parallel or perpendicular to each other. Their mutual orientation only weakly affected the efficiency of the modulation transfer, because, in contrast to the harmonic generation, the induced changes in the absorption in the medium were important for this effect, so that no spatial synchronism of the interacting waves was necessary. In the experiment, the spectra of the probe wave were recorded at 1-s intervals, which allowed us to compare the variations of the fundamental harmonic and the modulation lobes in time. An additional vibrator immersed in the medium generated short (1–10 ms) shock pulses, which produced perturbations in the medium. Figure 8 shows the time dependences of the amplitude of the fundamental (with the carrier frequency) component of the probe wave and the amplitudes of the induced first- and second-order combination components. In the course of these measurements, several pulses perturbing the medium were emitted (the instants of the pulse generation are indicated by arrows). Figure 8 demonstrates the

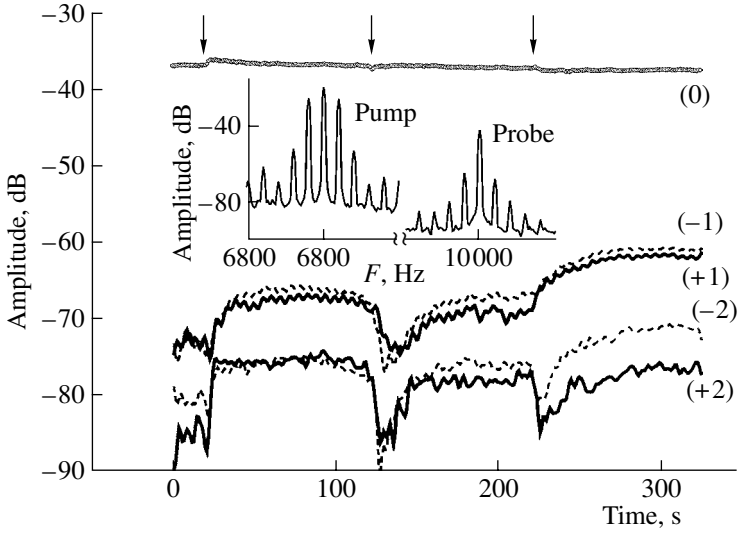

Fig. 8. Time dependences (at a step of 1 s) of the fundamental harmonic amplitude of the probe wave (marked with number 0) and of its right-hand and left-hand first- and second-order modulation lobes (marked with numbers ±1 and ±2). The arrows indicate the instants of "seismic events." The inset shows examples of the spectra of the 100% amplitude-modulated pump wave and the probe wave with induced modulation after their transmission through the medium.

difference in the sensitivity of the level variations for the modulation components and the fundamental harmonic: for the latter, these variations are very small. An important feature of the variations induced by the shock pulses in the cross-modulation components of the probe wave is their transient nature with a pronounced slow dynamics. The dynamics of these variations is determined by the gradual structural relaxation of the material within 1–70 s after the perturbing pulse (see Fig. 8). The inset to Fig. 8 shows the spectra of the pump and probe waves. Note that the higher modulation components appeared in the spectrum of the pump wave as a result of its propagation through the medium, and the shape of the spectrum of the probe wave does not reproduce the shape of the pump spectrum. For example, in the probe wave spectrum, the level of the second-order components may in some cases be equal to the level of the first-order components or even exceed it (as in Fig. 8 after the first perturbing pulse). Thus, the observed high sensitivity of the cross-modulation effects to small structural changes in the granular medium and, especially, to the structural relaxation processes can be effectively used, along with other nonlinear effects, for nondestructive testing of the state of a granular medium.

CONCLUSIONS

The results of the experimental studies described above testify that the nonlinear effects occurring in a granular medium are selectively sensitive to the presence of weak contacts (in contrast to linear elastic characteristics, for which the contribution of strong contacts predominates). The transition from the square law to the 3/2-power law in the amplitude dependence of the demodulated pulse and the beatings of the second harmonic with increasing amplitude of the primary shear wave suggest that the medium contains a considerable fraction of weak contacts (according to estimates, 60–70% of the total number of contacts). These nonlinear effects observed for shear waves made it possible to investigate the law of the dynamic dilatancy using the dependence of the amplitude of the demodulated signal on the shear pump amplitude. The characteristic features of the effects under study testify that the distribution function of intergrain contact forces noticeably increases in the region of small forces, much smaller than the mean contact force. For grains of irregular shape, such an increase near a zero force value is still more pronounced, because, for example, in dry sand, the square-law part of the amplitude dependence of the demodulated signal is practically absent [23]. These conclusions agree qualitatively with the recent results of the three-dimensional modeling of intergrain forces on the basis of the molecular dynamics approach [7]. For unloaded packings with allowance for friction, the modeling revealed a pronounced growth of the function $P = P(f)$ for $f \leq 10^{-1} f_0$. The results obtained should stimulate further theoretical modeling and experimental investigations of the elastic and inelastic behavior of granular materials.

The observed high sensitivity of nonlinear effects to the structure of a granular medium suggests good prospects for diagnostic applications of these effects in laboratory conditions and in seismic monitoring systems (where, in particular, the use of the acoustical analog of the Luxemburg–Gorki cross-modulation effect, which consists in the amplitude modulation transfer from an intense pump wave to a probe harmonic wave, may be of special interest).

ACKNOWLEDGMENTS

This work was supported in part by the Russian Foundation for Basic Research (project no. 05-05-6491) and the Program of the Division of Physical Sciences of the Russian Academy of sciences "Coherent Acoustic Fields and Signals." The experiments were carried out at the Acoustic Laboratory of Université du Maine (France) under the project PECO-NEI no. 16366.

REFERENCES

1. H. M. Jaeger, S. R. Nagel, and R. P. Behringer, Rev. Mod. Phys. **68**, 1259 (1996).
2. D. L. Blair *et al.*, Phys. Rev. E **63**, 041304 (2001).
3. G. Løvoll, K. J. Måløy, and E. G. Flekøy, Phys. Rev. E **60**, 5872 (1999).
4. C.-H. Liu *et al.*, Science **269**, 513 (1995).
5. F. Radjai and M. Jean, Phys. Rev. Lett. **77**, 274 (1996).
6. S. Luding, Phys. Rev. E **55**, 4720 (1997).
7. L. E. Silbert, G. S. Grest, and J. W. Laundry, Phys. Rev. E **66**, 061303 (2002).
8. V. Yu. Zaĭtsev, Akust. Zh. **41**, 439 (1995) [Acoust. Phys. **41**, 385 (1995)].
9. I. Yu. Belyaeva and V. Yu. Zaĭtsev, Akust. Zh. **43**, 594 (1997) [Acoust. Phys. **43**, 510 (1997)].
10. V. Yu. Zaĭtsev, A. B. Kolpakov, and V. E. Nazarov, Akust. Zh. **41**, 347 (1999) [Acoust. Phys. **45**, 305 (1999)].
11. V. Zaitsev, V. Gusev, and B. Castagnede, Phys. Rev. Lett. **89**, 105502 (2002).
12. L. D. Landau and E. M. Lifshitz, *Theory of Elasticity*, 4th ed. (Nauka, Moscow, 1986; Pergamon, Oxford, 1986).
13. V. Tournat, V. Zaitsev, V. Gusev, *et al.*, Phys. Rev. Lett. **92**, 085502 (2004).
14. B. K. Novikov, O. V. Rudenko, and V. I. Timoshenko, *Nonlinear Hydroacoustics* (Sudostroenie, Leningrad, 1981) [in Russian].
15. O. Reynolds, Philos. Mag. **20**, 469 (1885).
16. J. D. Goddard and A. K. Didwania, Q. J. Mech. Appl. Math. **51**, 15 (1998).
17. L. K. Zarembo and V. A. Krasil'nikov, *Introduction to Nonlinear Acoustics* (Nauka, Moscow, 1966) [in Russian].
18. D. Kolymbas *et al.*, Int. J. Numer. Anal. Met. Geomech. **19**, 415 (1995).
19. M. F. Hamilton, Yu. A. Ilĭnskii, and E. A. Zabolotskaya, *Nonlinear Acoustics*, Ed. by M. F. Hamilton and D. T. Blackstock (Academic, San Diego, 1997), pp. 151–175.
20. V. Tournat, V. Gusev, V. Zaitsev, and B. Castagnede, Europhys. Lett. **66**, 798 (2004).
21. V. L. Ginzburg, Izv. Akad. Nauk SSSR, Ser. Fiz. **12**, 253 (1948).
22. A. L. Bagmet, V. E. Nazarov, A. V. Nikolaev, *et al.*, Dokl. Ross. Akad. Nauk **346** (3), 390 (1996).
23. V. Zaitsev, V. Nazarov, V. Tournat, *et al.*, in *Proceedings of Joint Congress SFA/DAGA-04* (Strasbourg, 2004), p. 553.
24. V. Zaitsev, V. Nazarov, V. Tournat, *et al.*, Europhys. Lett. **70**, 607 (2005).

Translated by E. Golyamina